Available online at www.sciencedirect.com
ScienceDirect
Proceedings of the Combustion Institute 31 (2007) 1393–1400
Proceedings of the Combustion Institute
www.elsevier.com/locate/proci

The quenching of premixed turbulent flames of iso-octane, methane and hydrogen at high pressures

D. Bradley *, M. Lawes, Kexin Liu, R. Woolley

School of Mechanical Engineering, University of Leeds, Leeds LS2 9JT, UK

Abstract

Experimental and theoretical studies are reported of turbulent flame quenching, with premixed flames of methane–air, iso-octane–air and hydrogen–air. Mixtures were exploded in a fan-stirred explosion bomb in which the rms turbulent velocity was varied by changes in fan speed. Influences of Markstein number, pressure up to 1.5 MPa, and Karlovitz stretch factor, K, were studied. It was found that the ratio of the positive stretch rate for extinction of the laminar flame to the rms turbulent strain rate was an important parameter. Probabilities of flame propagation, p_f, from an initial kernel were measured. The conditions for probabilities of 0.8 and 0.2 were correlated in terms of the Karlovitz stretch factor and Markstein number. However, at a given p_f, the theoretical probability, P_{bf}, that the spectrum of stretch rates for a turbulent flame would support propagation, declined with increase in K. This theoretical probability assumed a positive flame stretch rate for quenching equal to that for the extinction of a steady-state laminar flame. Its declining value with K, at constant p_f, was attributed, at least in part, to the inability of non-steady-state flamelets of the turbulent flame to respond to transient excursions of flame stretch rates to values in excess of those that extinguish laminar flames. Another possibility was that the highly convoluted flames were able to follow a route through regions of sufficiently low stretch rate to avoid extinctions.

Keywords: Turbulent flames; Quenching; High pressure; Stretch rate

1. Introduction

Information on the quenching of turbulent flames at high pressure is important for the design of practical combustors and for improved fundamental understanding of turbulent combustion. The increased flame stretch rate arising from turbulence narrows the bounds for turbulent combustion. Earlier experimental studies of turbulent premixed flame quenching [1–3], have covered a variety of mixtures but were limited to atmospheric pressure. The findings were collated in [3] in terms of the Karlovitz stretch factor, K, and Lewis number, Le, for flame quenching. Subsequent direct numerical simulations of quenching [4] were in general agreement with these experimental findings. It was assumed in [4] that the quenched parts of the flame had no influence upon the active parts. In the quenched parts burned gas was penetrated by reactants and cooled by them. This cooling might be sufficient to induce localised quenching, but this was difficult to quantify.

Another computational study [5] demonstrated a maximum value of the turbulent burning velocity, u_t, as the turbulence increased, followed, in the presence of mild heat loss, by flame extinction.

* Corresponding author. Fax: +44 113 343 2150.
E-mail address: d.bradley@leeds.ac.uk (D. Bradley).

1540-7489/$ - see front matter
doi:10.1016/j.proci.2006.07.022

Effects of radiative heat loss from CH_4–air flames were studied experimentally in [6] at atmospheric pressure, using a cruciform burner. Critical values of K for global quenching were found, with control of radiative loss by N_2 and CO_2 dilution. For lean mixtures dilution with CO_2 reduced such critical values and this was attributed to increased radiative loss. There was no comparable effect for rich mixtures.

The introduction of Le into the correlations in [3] was an attempt to allow for thermo-diffusive influences on flame propagation and quenching. Various theoretical analyses, including [7,8] have suggested that the Markstein number for strain rate, Ma_{sr} is a more fundamental parameter. There is, for example, but a small change in Le between lean and rich CH_4–air mixtures, compared with that in Ma_{sr} [7], even though the critical values of K differ [6]. Furthermore, as will be shown, critical values of K are pressure dependent yet Le, unlike Ma_{sr}, has little pressure dependency. Mixtures with negative values of Ma_{sr}, allied to large stretch rates for flame extinction, are particularly difficult to quench [7]. The present experimental and theoretical studies explore the influences of laminar flame extinction stretch rates and high pressure on turbulent flame quenching. A variety of mixtures were exploded in a fan-stirred explosion bomb, up to the point of flame extinction. Only with very rich iso-octane–air mixtures that produced sooting flames and near-limit H_2–air flames were radiative losses significant. The compositional changes principally affected the laminar burning velocity, u_ℓ, extinction stretch rate, and Ma_{sr}.

2. Apparatus

The spherical stainless steel bomb, internal radius 193 mm, had three pairs of orthogonal windows. Reasonably uniform isotropic turbulence was created by four identical fans, symmetrically disposed in a regular tetrahedron configuration, located close to the bomb wall. Each fan was driven by a directly coupled electric motor with a separate speed control. Turbulent parameters of the initial mixture were measured by laser doppler velocimetry. The rms turbulent velocity, u', increased linearly with fan speed and was independent of pressure. The longitudinal integral length scale, $L = 20$ mm, was found by two point correlation and was independent of pressure and fan speed.

It was not possible to generate sufficiently high values of u' to extinguish all flames. In [9] atmospheric, stoichiometric flames of propane and hydrogen could not be extinguished, even with the maximum attainable value of u' of 17 m/s. In the present study, because of the high pressures, the fan shaft sealing requirements were more stringent and this restricted the fan speed to a maximum of 8500 rpm, ($u' = 10$ m/s).

Pressures were measured with a Kistler 701 pressure transducer. Energies of about 26 mJ (from a 12 V automotive coil) were supplied to a central spark gap of 1 mm. Flame fronts were observed by high speed schlieren ciné-photography. Mixtures of iso-octane–air, methane–air, hydrogen–air and methane/hydrogen–air were electrically heated to an initial temperature of 365 K, over a range of initial pressures between 0.1 and 1.5 MPa. A flame kernel formed around the spark and in some instances it propagated throughout the bomb, while in others it quenched. If flame quenching occurred, it always did so in the first stage of constant pressure burning. Several explosions were attempted under identical initial conditions. The fraction of the initial flame kernels that propagated throughout the bomb was the probability of flame propagation, p_f.

3. Theory

The analysis in [7] and [8] expresses the mean volumetric heat release rate, $\bar{q}_t$, in terms of local values of heat release rate in an unstretched laminar flame, $q_{\ell 0}(c)$, where c is a reaction progress variable and its pdf is $p(c)$, by:

$$\bar{q}_t = P_b \int_0^1 q_{\ell 0}(c)p(c)\mathrm{d}c. \quad (1)$$

The burning rate factor, P_b, covers the influences of flame stretch rate and is:

$$P_b = \int_{s_{q-}}^{s_{q+}} f(s)p(s)\mathrm{d}s. \quad (2)$$

Here, s is a dimensionless flame stretch rate, the stretch rate multiplied by the Kolmogorov time, $(\lambda/(u'15^{1/2}))$, where λ is the Taylor scale of turbulence. Its pdf is $p(s)$, is derived in [8] in terms of K, the turbulent Reynolds number, R_L, and Ma_{sr}. The expression for it is given in [7]. K is defined by:

$$K = (\delta_\ell/u_\ell)(u'/\lambda), \quad (3)$$

where δ_ℓ is the laminar flame thickness, given by ν/u_ℓ, with ν the kinematic viscosity, and λ is related to L by $\lambda/L = (A/R_L)^{1/2}$, where A is a numerical constant = 16. These yield:

$$K = 0.25(u'/u_\ell)^2/R_L^{1/2}. \quad (4)$$

The flame stretch factor $f(s)$ expresses the influence of s on $q_{\ell 0}(c)$, so that the stretched heat release rate is $f(s)q_{\ell 0}(c)$. It varies linearly with s and is expressed in [7] in terms of K, Ma_{sr} and the unburned/burned gas density ratio, ρ_u/ρ_b. The integral limits are s_{q+} and s_{q-}, the dimensionless flame extinction stretch rates under positive and negative flame stretch rates in laminar flam-

elets. Values of the positive stretch rate for laminar flame extinction, $\alpha_{q\ell+}$, have been derived from experiment [10] and chemical kinetic laminar flame modeling [11], almost exclusively at atmospheric pressure and for only a limited range of mixtures. Consequently, following [12], it was necessary to obtain the greatest possible degree of generality from the somewhat meager data available. This was partially achieved by multiplying the available values of $\alpha_{q\ell+}$ by the chemical time, δ_ℓ/u_ℓ, to yield a laminar Karlovitz stretch factor for flame extinction, $K_{q\ell+} = \alpha_{q\ell+}(\delta_\ell/u_\ell)$. When $\alpha_{q\ell+}$ is multiplied by the Kolmogorov time and a small term added to allow for the "burned to unburned" flamelet correction [7,12],

$$s_{q+} = K_{q\ell+}/(K15^{1/2}) - 0.014/15^{1/2}. \quad (5)$$

Values of $K_{q\ell+}$ are presented in [7]. These were derived from those of $\alpha_{q\ell+}$ measured in [10] for full ranges of ϕ, equivalence ratio, for CH_4–air and C_3H_8–air mixtures, under atmospheric conditions. There was less spread in the values of $K_{q\ell+}$ than in those of $\alpha_{q\ell+}$. The values of $K_{q\ell+}$ increased appreciably as Ma_{sr} became negative and gave a continuous curve when plotted against Ma_{sr}. This curve was employed for all the hydrocarbon mixtures in the present work, to give $K_{q\ell+}$ for the known, or estimated, value of Ma_{sr} for a given mixture. For very lean hydrogen mixtures, values of $\alpha_{q\ell+}$ in [11] yielded those of $K_{q\ell+}$ which, similarly were plotted against Ma_{sr}. This relationship was different from that for the hydrocarbons.

The situation is even more uncertain for extinction by negative stretch rates, for which unstable flames there are negligible data. The procedure was to prescribe negative burning velocities, which led to [7]:

$$s_{q-} = [(\rho_u/\rho_b - 1)CMa_{sr}K]^{-1}, \quad (6)$$

in which $C = -0.48$ if Ma_{sr} is positive and 4.7 if Ma_{sr} is negative. For $Ma_{sr} = 0$, s_{q-} was taken to be $-2.5s_{q+}$.

As u' increases, fractal considerations of the increased flame wrinkling suggest how the turbulent burning velocity, u_t, also increases. The associated increased flame stretch rates lead to increasing extinctions in local flamelets. Initially, the first trend predominates, but at the highest values of u' the latter one does, until eventually the flame globally quenches. Consideration of these factors in [7] led to the relationship between u_t and u'_k, the effective rms velocity acting on the flame front:

$$\frac{u_t}{u'_k} = \left(\frac{u_\ell}{u'_k} + F\right)P_b^{0.5} \text{ for } u_\ell/u'_k \leqslant 1.0. \quad (7)$$

F is a factor dependent upon the Kolmogorov and turbulent dissipation constants and lies in the range 2.3 ± 0.15. Clearly, as $P_b \to 0$ the flame will quench and evaluation of P_b provides a criterion for turbulent flame quenching. However, in Eq. (2) the factor $f(s)$ is essentially a modifier of the burning rate, rather than an indicator of flame propagation. The latter is conveniently expressed by a flame propagation probability:

$$P_{bf} = \int_{s_{q-}}^{s_{q+}} p(s)\mathrm{d}s. \quad (8)$$

This is the probability that the stretch rates to which a turbulent flame is exposed will support flame propagation. It is not the same as the probability of an initial flame kernel continuing to propagate, p_f. Nevertheless, some relationship between the two is to be expected, with the two increasing and decreasing in harmony. Insight into quenching mechanisms will be obtained by comparing experimental values, p_f, with the theoretical values, P_{bf}.

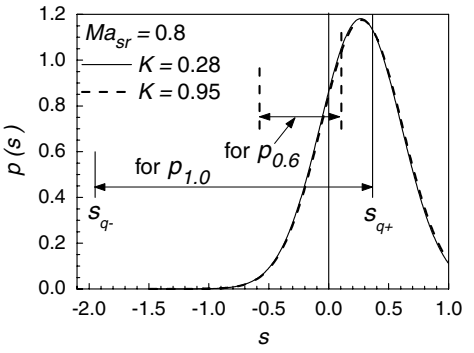

Fig. 1. Ranges of stretch rates on $p(s)$ curve for $p_{1.0}$ ($K = 0.28$) and $p_{0.6}$ ($K = 0.95$) that allow of flame propagation.

Shown on Fig. 1 is part of the $p(s)$ curve for an iso-octane–air mixture, $\phi = 0.8$, at 1.0 MPa and 365 K, for the experimental values of u' at $p_{0.6}$ and at the limit $p_{1.0}$. The corresponding values of K are 0.95 and 0.28, respectively. An experimental value of $Ma_{sr} = 0.8$ [19], yielded $K_{q\ell+} = 0.40$. In this instance $p(s)$ is relatively insensitive to the different values of K and R_L. The limits of the integral in Eq. (8) between s_{q+} and s_{q-} are narrowed as $p_{1.0}$ decreases to $p_{0.6}$, as K increases. All values of Ma_{sr} and u_ℓ employed are given in Table 1, along with the symbol employed for each mixture, with the pressure indicated by internal lines.

4. Experimental and derived results

Figure 2a shows the measured variations of p_f with u' for iso-octane–air mixtures, $\phi = 0.8$, 2.0 and 2.5, at pressures of 0.5, 1.0 and 1.5 MPa. It was not possible to quench the flames at all between $\phi = 1.5$ and 2.0, a regime of negative

Table 1
Physico-chemical properties employed

Mixture	Symbol	P (MPa)	u_ℓ (m/s)	Ma_{sr}	$K_{q\ell+}$	Le
CH_4–air (ϕ)						
0.55	⊖	0.5	0.026* [13–15]	−0.3* [13]	1.10	1.01
	⊕	1.0	0.014* [13,14]	−2.2* [13]	1.90	1.01
0.60	△	0.1	0.189 [13–15]	2.0 [15]	0.29	1.01
	⟁	0.5	0.058 [13]	−0.2 [13]	1.00	1.01
	⟁	1.0	0.034* [13,14]	−2.0* [13,15]	1.90	1.01
0.65	☆	0.5	0.090* [13]	−0.1* [13]	0.90	1.01
	✱	1.0	0.057* [13,14]	−2.1* [13]	1.90	1.01
1.25	⊖	0.5	0.180* [13–15]	4.8* [13]	0.16	1.09
1.30	⊟	0.5	0.130 [13]	5.4 [13]	0.15	1.09
	⊞	1.0	0.087* [13,14]	2.6* [13,15]	0.30	1.09
1.35	⊳	0.5	0.095* [13]	6.0* [13]	0.15	1.09
	⊳	1.0	0.063* [13,14]	2.9* [13]	0.22	1.09
i-C_8H_{18}–air (ϕ)						
0.80	⊖	0.5	0.201 [13]	5.0 [19]	0.15	2.97
	⊕	1.0	0.162 [13]	0.8 [19]	0.40	2.97
	⊗	1.5	0.131* [13]	−1.0* [19]	1.8	2.97
1.20	◁	0.1	0.40 [9]	0.8 [19]	0.40	0.93
1.00	◁	0.1	0.446 [9]	5.3 [19]	0.15	1.43
0.92	◁	0.1	0.42 [9]	8.1 [19]	0.10	2.95
0.85	◁	0.1	0.393 [9]	11.0 [19]	0.10	2.98
H_2–air (ϕ)						
0.15	▽	0.1	0.087* [16,17]	−1.5* [16]	<0.03 [11]	0.36
	⩛	0.5	0.036* [16,17]	−2.0* [16]	<0.03 [11]	0.36
	⩛	1.0	0.027* [16,17]	−2.5* [16]	<0.03 [11]	0.36
	⊠	1.5	0.020* [16,17]	−3.0* [16]	<0.03 [11]	0.36
C_3H_8–air (ϕ)						
0.70	◇	0.1	0.300 [9]	6.2 [18]	0.11	2.03
0.80	◇	0.1	0.390 [9]	6.0 [18]	0.15	1.98
0.90	◇	0.1	0.466 [9]	6.1 [18]	0.16	1.97

Notes. References are given in brackets. A value followed by an asterisk is an estimate based on given references.

Ma_{sr} and high $K_{q\ell+}$. For $\phi \geqslant 2.0$, the flames were thick and very sooty and eventually quenched at $\phi = 2.5$. Variations of p_f with u' for the lean methane–air mixtures, $\phi = 0.55$, 0.60, 0.65 and 0.70, are shown in Fig. 2b. It was not possible to quench flames for $\phi \geqslant 0.7$, until a value of 1.25 was reached, at which $K_{q\ell+}$ became smaller. Results for the rich methane mixtures, $\phi = 1.2$, 1.25, 1.3 and 1.35, at pressures up to 1.0 MPa are presented in Fig. 2c.

For the near-limit hydrogen mixtures, quenching only became possible when ϕ was reduced to 0.15. With a further slight decrease to 0.10 the flammability limit was reached when the pressure was increased to 0.5 MPa. Data for $\phi = 0.15$ at four different pressures up to 1.5 MPa are given by the full line curves in Fig. 2d. Data for a lean, $\phi = 0.6$, mixture of 0.1 H_2/0.9 CH_4–air are shown by the broken curves at three pressures.

Values of P_{bf}, given by Eq. (8) for the experimental values of K, R_L and Ma_{sr}, are plotted against K at different pressures in Fig. 3, for the different mixtures. Lack of data on u_ℓ, Ma_{sr} and $K_{q\ell+}$ prevents analysis of the two rich iso-octane–air flames. There is a particular problem for negative values of Ma_{sr} because the very unstable laminar flames make such measurements difficult. Each isobar in Fig. 3 decreases from an upper limit value of p_f of unity down to the lowest measured value, usually 0. Locations of the $p_{0.8}$ and $p_{0.2}$ points are indicated by half-shaded and full-shaded symbols, respectively. As expected, an increase in K decreases both p_f and P_{bf}.

In Fig. 3a some data for iso-octane–air at higher values of u' than were attainable in the present rig are taken from [9]. For the hydrocarbon mixtures, in general, as the pressure *increases*, Ma_{sr} decreases and $K_{q\ell+}$ *increases*. Consequently, see Eq. (5), s_{q+} increases, as does P_{bf}, see Eq. (8). Hence a higher value of K is necessary at the higher pressure to produce the same degree of quenching. This can be seen from the $p_{0.8}$ and $p_{0.2}$ points on the isobars in Figs. 3a–c.

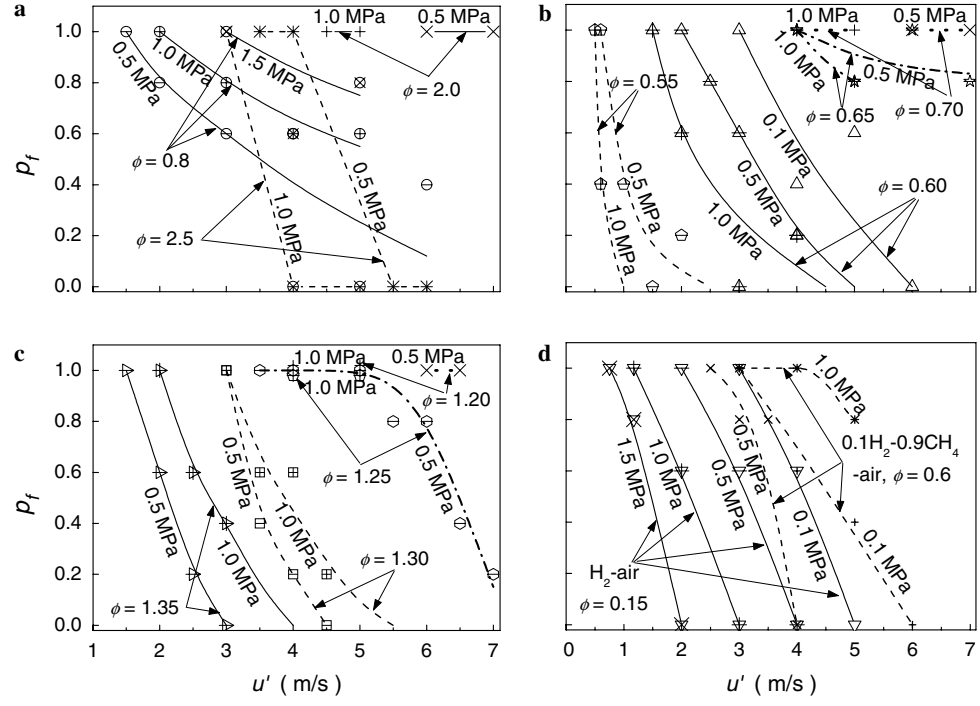

Fig. 2. Experimental variation of p_f with u' for different mixtures at different pressures. (a) Iso-octane–air, (b) lean CH_4–air, (c) rich CH_4–air, (d) H_2–air and 0.1 H_2–0.9 CH_4–air.

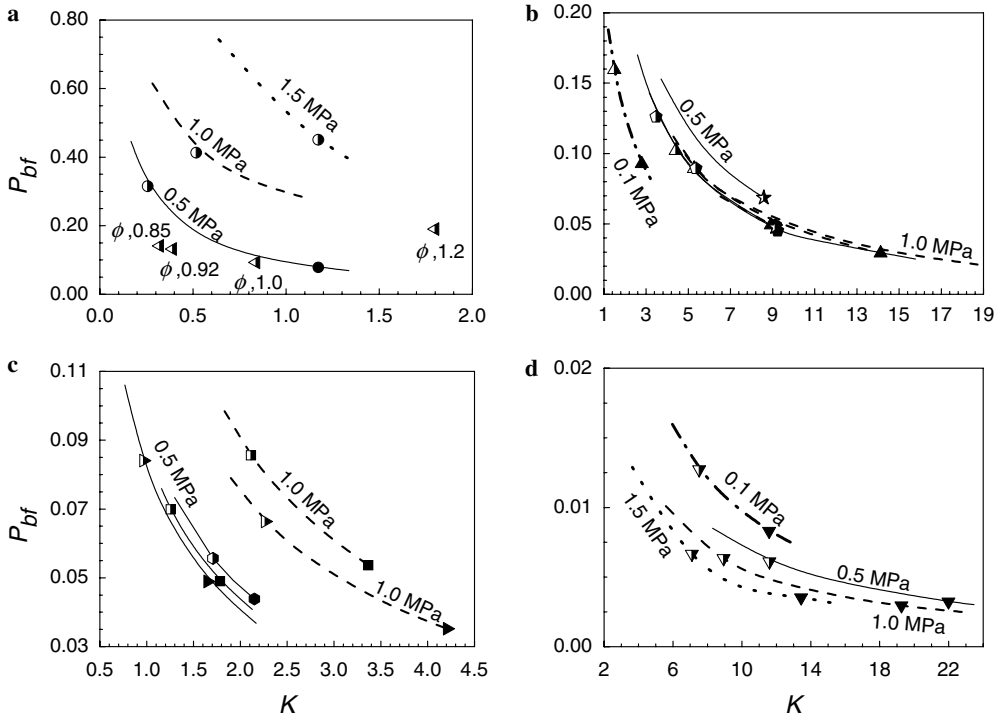

Fig. 3. Theoretical values, P_{bf}, for different values of K. Experimental quenching is indicated by half-shaded and full-shaded symbols for $p_{0.8}$ and $p_{0.2}$ points. (a) Iso-octane–air, (b) lean CH_4–air, (c) rich CH_4–air, (d) H_2–air $\phi = 0.15$.

In contrast, for the near-limit H_2–air mixture, $\phi = 0.15$, as the pressure increases, $K_{q\ell+}$ *decreases* [11] (up to the point of complete extinction for $\phi = 0.1$ at 0.5 MPa). Hence s_{q+} must also decrease, as must P_{bf}. In addition, u_ℓ decreases, increasing K. As the extinction limit is approached $K_{q\ell+}/K \to 0$, $s_{q+} \to 0$, and $P_{bf} \to 0$. This explains the very low values of P_{bf} at high K in Fig. 3d. The ratio $K_{q\ell+}/K(= \alpha_{q\ell+}/(u'/\lambda))$ is the positive stretch rate for extinction of the laminar flame, normalised by the rms turbulent strain rate. For the hydrocarbon mixtures, the minimum value of the ratio is about 0.083. For H_2–air, $\phi = 0.15$, it is less than 0.005.

5. Discussion

Shown in Fig. 4 are data points for P_{bf}, at all the measured $p_{0.8}$ conditions for hydrocarbon mixtures, plotted against $K/K_{q\ell+}$, for which the full line curve is the best fit. The dashed curve is the best fit to the $p_{0.2}$ points (not shown). The decline of P_{bf} at constant p_f suggests that the theoretical approach that led to Eq. (8), increasingly over-estimates the extent of flamelet quenching. Uncertainties in thermo-chemical data might partially explain this. There is certainly an urgent need for more accurate values of laminar flame extinction stretch rates, for positive and negative stretch, at high pressures.

A second explanation is that, although at low values of K, flame kernels are approximately spherical, as K increases, they depart from this geometry, as flames propagate through regions that are less highly aerodynamically strained. This bias towards lower stretch rates could explain the co-existence of high values of p_f with low values of P_{bf}.

A third explanation is that, whereas $\alpha_{q\ell+}$, and hence s_{q+}, is found from steady-state laminar flames, the laminar flamelets of turbulence are increasingly far from steady as K increases. Theoretical studies indicate that oscillatory laminar flames are increasingly unable to respond to higher frequencies [20]. Optical diagnostics of turbulent flames show that flamelet surfaces do not always quench locally during brief excursions of the local stretch rate to values above $\alpha_{q\ell+}$ [21]. In [7] it is suggested that the departure from quasi-steady conditions increases with $(K/K_{q\ell+})^{1/2}$. It therefore is postulated that P_{bf} is inversely proportional to $(K/K_{q\ell+})^{1/2}$. Application of this inverse square root law to the $p_{0.8}$ condition generates a relationship of the form shown by the dotted curve on Fig. 4. Its closeness to the observed relationship supports the explanation in terms of increasing resistance to flame quenching at higher frequencies.

At the highest pressures, the addition of H_2 to CH_4–air mixtures suppresses quenching, as can be seen from Fig. 2d. For $\phi = 0.6$, 1.0 MPa, the presence of 10% H_2 in the fuel increased u' at $p_{0.8}$, from 1.8 to 5 m/s.

The search for empirical correlations of the results led to the plot of Ma_{sr} against K for $p_{0.8}$ and $p_{0.2}$ in Fig. 5. The symbols indicate experimental points for $p_{0.8}$ only, obtained from the curves in Fig. 2. The best fit curves to these points give: for $-3.0 \leqslant Ma_{sr} \leqslant 11.0$

$$\text{(a) } K(Ma_{sr}+4)^{1.8} = 34.4 \text{ for } p_{0.8} \text{ and}$$
$$\text{(b) } K(Ma_{sr}+4)^{1.4} = 37.1 \text{ for } p_{0.2}. \quad (9)$$

Whether a given value of p_f is attained for fixed turbulent parameters depends on Ma_{sr} and u_ℓ. For the

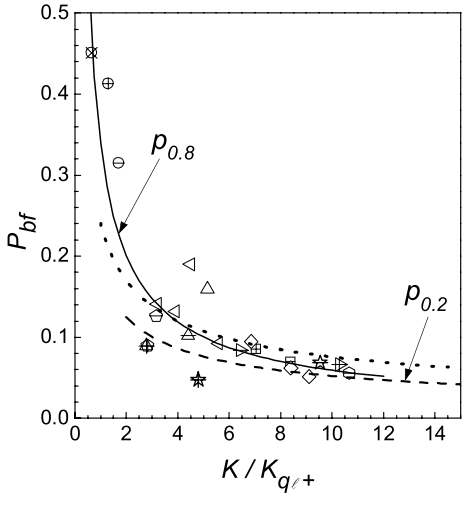

Fig. 4. Values of P_{bf} at all $p_{0.8}$ conditions for listed mixtures, plotted by full line curve. Values for $p_{0.2}$ conditions given by dashed curve, (points not shown). Dotted curve shows inverse square root law for $p_{0.8}$.

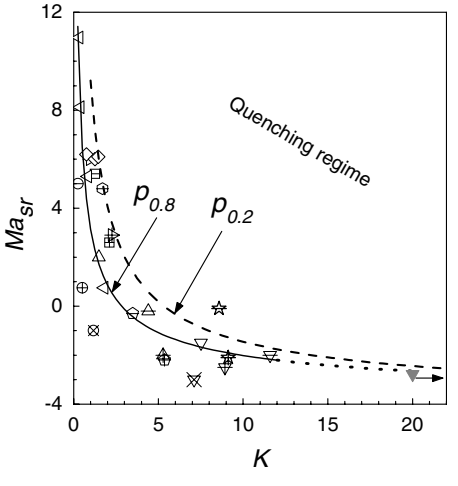

Fig. 5. Values of K, for measured $p_{0.8}$ and $p_{0.2}$, at different Ma_{sr}. Symbols are for $p_{0.8}$ points only.

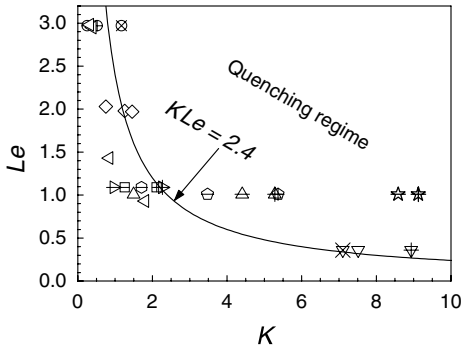

Fig. 6. Values of K, for measured $p_{0.8}$, at different values of Le.

same p_f, Fig. 5 shows that a decrease in Ma_{sr} increases K. If this change is accompanied by an increase in u_ℓ then K falls to less than its original value, with a consequent increase in p_f. Conversely, when both Ma_{sr} and u_ℓ decrease, so does p_f.

Decreases in Ma_{sr} and increases in u_ℓ occurred with the H_2–air mixture when ϕ was increased from 0.15 to 0.2. The consequent increase in p_f to unity was such that even when u' was increased to the maximum attainable value of 10 m/s there was still no flame quenching. The grey triangle symbol in Fig. 5 is for H_2–air, $\phi = 0.2$ and 0.1 MPa, $Ma_{sr} = -2.8$, with $u' = 10$ m/s. The $p_{0.8}$ point must be at a higher value of K, as suggested by the arrow.

For $R_L \geqslant 300$ a quenching law was proposed in [3]. This was based on a different value of A and, with the present value, the law is $K = 2.4/Le$ for $p_{0.8}$, plotted in Fig. 6. Unlike Ma_{sr}, Le does not change with pressure and it can be seen that for the same value of Le at different pressures there is a wide range of K values for $p_{0.8}$. Consequently, predictions of critical values of K are less sensitive and less accurate than those based on Ma_{sr}.

6. Conclusions

Following the theoretical guidelines, the influences of Ma_{sr}, pressure, and K on turbulent flame quenching have been studied experimentally in a previously unexplored regime covering a wide range of Ma_{sr}, and pressures up to 1.5 MPa. Eqs. (9) (a) and (b) express measured critical Karlovitz stretch factors as a function of Ma_{sr}. The dearth of accurate physico-chemical data, particularly when the corresponding laminar flames are unstable, limits the accuracy of these generalizations and they may be more general than is warranted. Nevertheless, they are an advance on a previous one, particularly with regard to pressure dependency. The addition of H_2 to CH_4 appears to be effective in delaying the onset of turbulent flame quenching at high pressure.

The experimental results suggest that as K increases, the main limitation in the theory is the assumption of steady-state stretch extinction values, and a consequent over-estimation of flamelet quenching. In addition, at high values of K, a flame might preferentially follow a route through regions of low stretch rate. The inability of non-steady-state flamelets to respond to transient excursions of flame stretch rates to values in excess of those that extinguish laminar flames is given some support by the observed variation of P_{bf} with $K/K_{q\ell+}$ for a given p_f.

Acknowledgments

The support of EPSRC, Shell Global Solutions and Siemens Industrial Turbomachinery is gratefully acknowledged.

References

[1] V.P. Karpov, A.S. Sokolik, *Proc. Acad. Sci. USSR, Phys. Chem. Sec.* 141 (1961) 866–869.
[2] J. Chomiak, J. Jarosiński, *Combust. Flame* 48 (1982) 241–249.
[3] R.G. Abdel-Gayed, D. Bradley, *Combust. Flame* 62 (1985) 61–68.
[4] C. Meneveau, T. Poinsot, *Combust. Flame* 86 (1991) 311–332.
[5] L. Kagan, G. Sivashinsky, *Combust. Flame* 120 (2000) 222–232.
[6] S.I. Yang, S.S. Shy, *Proc. Combust. Inst.* 29 (2002) 1841–1847.
[7] D. Bradley, P.H. Gaskell, X.J. Gu, A. Sedaghat, *Combust. Flame* 143 (2005) 227–245.
[8] D. Bradley, P.H. Gaskell, X.J. Gu, A. Sedaghat, *Combust. Flame* 135 (2003) 503–523.
[9] R.G. Abdel-Gayed, D. Bradley, M.N. Hamid, M. Lawes, *Proc. Combust. Inst.* 20 (1985) 505–512.
[10] C.K. Law, D.L. Zhu, G. Yu, *Proc. Combust. Inst.* 21 (1986) 1419–1426.
[11] Yufei Dong, A.T. Holley, M.G. Andac, F.N. Egolfopoulos, S.G. Davis, P. Middha, Hai Wang, *Combust. Flame* 142 (2005) 374–387.
[12] D. Bradley, A.K.C. Lau, M. Lawes, *Philos. Trans. R. Soc. Lond.* A338 (1992) 359–387.
[13] M.P. Ormsby, *Turbulent flame development in a high-pressure combustion vessel*, 2005, Ph.D. Thesis, University of Leeds.
[14] F.N. Egolfopoulos, P. Cho, C.K. Law, *Combust. Flame* 76 (1989) 375–391.
[15] D. Bradley, P.H. Gaskell, X.J. Gu, *Combust. Flame* 104 (1996) 176–198.
[16] S. Verhelst, R. Woolley, M. Lawes, R. Sierens, *Proc. Combust. Inst.* 30 (2005) 209–216.
[17] K.J. Al-Khishali, D. Bradley, S.F. Hall, *Combust. Flame* 54 (1983) 61–70.

[18] D. Bradley, P.H. Gaskell, X.J. Gu, *Proc. Combust. Inst.* 27 (1998) 849–856.
[19] D. Bradley, R.A. Hicks, M. Lawes, C.G.W. Sheppard, R. Woolley, *Combust. Flame* 115 (1998) 126–144.
[20] F.N. Egolfopoulos, C.S. Campbell, *J. Fluid. Mech.* 318 (1996) 1–29.
[21] J.M. Donbar, J.F. Driscoll, C.D. Carter, *Combust. Flame* 125 (2001) 1239–1257.